



**Calhoun: The NPS Institutional Archive**  
**DSpace Repository**

---

Department of Mechanical and Aerospace Engineering (MAE) Faculty and Researchers Collection

---

2005-08-15

# Optimal Trajectory of a Glider in Ground Effect and Wind Shear

Harada, Masanori; Bollino, Kevin

The American Institute of Aeronautics and Astronautics (AIAA)

---

<http://hdl.handle.net/10945/29669>

*Downloaded from NPS Archive: Calhoun*



Calhoun is a project of the Dudley Knox Library at NPS, furthering the precepts and goals of open government and government transparency. All information contained herein has been approved for release by the NPS Public Affairs Officer.

**Dudley Knox Library / Naval Postgraduate School**  
**411 Dyer Road / 1 University Circle**  
**Monterey, California USA 93943**

<http://www.nps.edu/library>

# Optimal Trajectory of a Glider in Ground Effect and Wind Shear

Masanori Harada\*

*National Defense Academy in Japan  
 1-10-20 Hashirimizu, Yokosuka 239-8686, Japan*

Kevin Bollino†

*Naval Postgraduate School, Monterey, CA, 93940*

The optimal, maximum range trajectory for a glider in ground effect and wind shear has been analyzed using numerical methods and analytical techniques based on optimal control theory. This investigation models the glider's nonlinear dynamics and includes both ground effect and wind shear models. An optimal control problem is formulated to maximize downrange distance and it includes state-variable inequality constraints. The problem is then solved using an algorithm that implements a Legendre pseudospectral collocation method. The results show that the glider's optimal trajectory follows an energy-efficient trajectory, the altitude path with the lowest energy height consumption in ground effect and tail-wind shear. The numerical results are presented within.

## Nomenclature

$b$	Wing Span, [m] (=15)
$C_L$	Lift Coefficient
$C_D$	Drag Coefficient
$C_{D0}$	Zero-Lift Drag Coefficient (=0.017)
$f_X, f_Z$	Force on Ground-Fixed Axis, [N]
$k$	Induced Drag Coefficient Factor (=0.018)
$h_e$	Energy Height [m]
$\dot{h}_e$	Energy Height Consumption [m/s]
$m$	Mass, [kg] (=300)
$S$	Wing Planform Area, [m <sup>2</sup> ]
$u$	Inertial Velocity, [m/s]
$u_a$	Airspeed, [m/s]
$u_w$	Wind Speed, [m/s]
$x, h$	Ground-Fixed Axis, [m]
$\gamma$	Flight Path Angle on Ground-Fixed Axis, [deg]
$\gamma_a$	Flight Path Angle on Air Axis, [deg]
$\rho$	Density, [kg/m <sup>3</sup> ]

## Introduction

**A**PPROACH and landing is a critical flight phase for an unpowered vehicle ( the glider ). For this reason, in trajectory optimization, it is important for the glider to use its own energy efficiently under the influence of external atmospheric disturbances such as wind. The desire for this efficient energy management is driving the research of guidance and control methods for approach and landing trajectories.<sup>1,2</sup>

It is well known that for a maximum range glide, consisting mostly of the approach phase, the lift-to-

drag ratio must be maximized. However, this may not be the optimal approach flight when considering the effects of wind. In real atmospheric flight, wind can potentially change the steady-state conditions imposed on the vehicle. Furthermore, the analysis can not neglect ground effect because it has an advantage of decreasing the induced drag at low altitude. For example, Azuma noticed that in cases of low initial energy, level flight at low altitudes in ground effect is better than steady-state gliding.<sup>3</sup> Trajectory analysis work of Kluever<sup>1</sup> included ground effect and wind, but in his model the wind speed was assumed constant. Since variation in wind speed close to the ground can significantly affect the glider's optimal range, modeling wind such that the speed varies with height (i.e. wind shear) is essential. In addition, in the presence of tail wind, the glider must fly at higher altitudes in order to preserve energy. Therefore, including the affects of wind variations and ground effect provides a trade-off height that must be accounted for in the optimal trajectory analysis.

The phenomena of trade-off height has been reported by the Daedalus Project,<sup>4</sup> but the literature shows that there has been limited numerical analysis involving both ground effect and wind shear. This is partially because the optimization of path-constrained nonlinear dynamic systems such as those arising in the guidance and control of gliders has long been considered a difficult problem. In the past, gliding flight was analyzed<sup>7-10</sup> using nonlinear optimal control methods<sup>5,6</sup> based strictly on calculus of variations. This research required the flight trajectory to be solved in segments due to divergence characteristics of the method. Also, it was difficult to handle state variable inequality constraints and it required large calculation

\*Lecturer, Department of Mechanical Engineering, AIAA member (Visiting Associate Professor, Department of Mechanical and Astronautical Engineering, Naval Postgraduate School.)

†Ph.D. Candidate, Department of Mechanical and Astronautical Engineering, AIAA member.

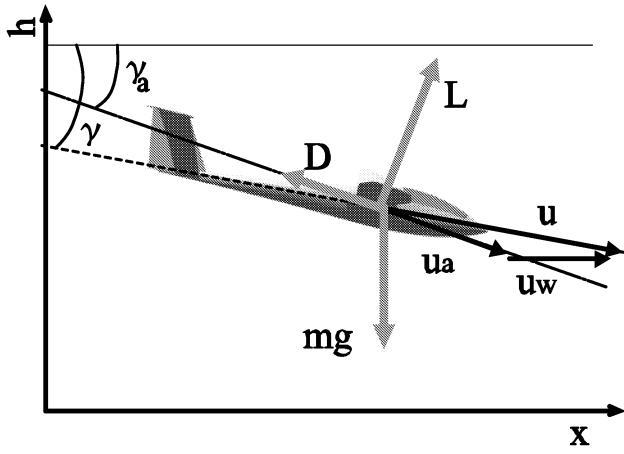


**Fig. 1 Coordinate System and Reference Frames of the Glider in Wind Shear**

time. Recently, more powerful numerical analysis techniques based on collocation methods were developed. Also, certain methods can now provide valuable information such as a Hamiltonian or co-state(s) that can verify optimality of a given solution.

In this paper, the optimal trajectory of a glider in ground effect and wind shear has been solved using a nonlinear optimal control analysis tool, DIDO,<sup>11</sup> which is based on a Legendre pseudospectral collocation method. The results show that the optimal trajectory follows the altitude which has the lowest energy consumption in ground effect and tail wind shear.

### Notation of Problem

The relevant reference frames used to describe the glider's position, orientation, and velocity are presented in Fig.1. Gliding is assumed to take place in a vertical plane over a flat Earth, and a coordinate system fixed to the ground is defined as the inertial reference frame. Only a wind speed component parallel to the ground surface is considered in this paper. Inertial velocity  $u$  refers to the ground-fixed axis and airspeed  $u_a$  to the air axis. The lift force  $L$  and the drag force  $D$  are transposed to the ground-fixed axis. On the basis of these assumptions and according to the free-body diagram in Fig.1, the equations of motion for the glider in ground effect and wind shear are given by Eq.(1)-(4).

$$m\dot{u} = f_X \cos \gamma + f_Z \sin \gamma - mg \sin \gamma \quad (1)$$

$$m u \dot{\gamma} = -f_X \sin \gamma + f_Z \cos \gamma - mg \cos \gamma \quad (2)$$

$$\dot{x} = u \cos \gamma \quad (3)$$

$$\dot{h} = u \sin \gamma \quad (4)$$

here

$$f_X = \frac{1}{2} \rho S u_a^2 (-C_L \sin \gamma_a - C_D \cos \gamma_a) \quad (5)$$

$$f_Z = \frac{1}{2} \rho S u_a^2 (C_L \cos \gamma_a - C_D \sin \gamma_a) \quad (6)$$

$$C_D = C_{D0} + k f(h) C_L^2 \quad (7)$$

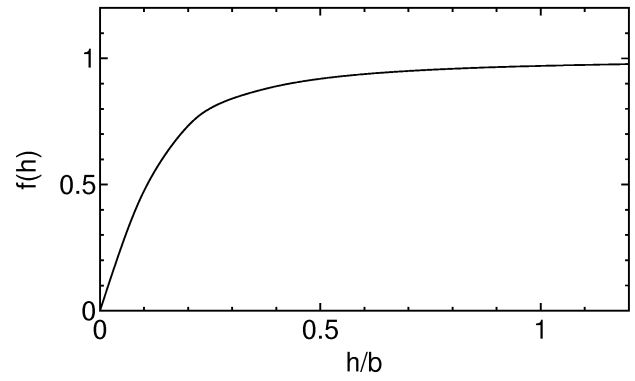


**Fig. 2 Ground Effect Factor of the Induced Drag Coefficient**

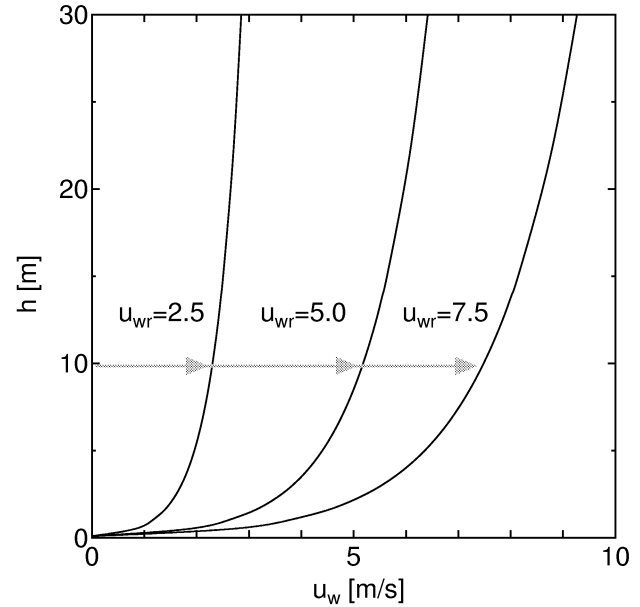


**Fig. 3 Profile of Wind Shear for Reference Height  $H_r = 10$ [m]**

$$u_a = \sqrt{(u \cos \gamma - u_w)^2 + (u \sin \gamma)^2} \quad (8)$$

$$\cos \gamma_a = \frac{u \cos \gamma - u_w}{u_a} \quad (9)$$

$$\sin \gamma_a = \frac{u \sin \gamma}{u_a} \quad (10)$$

### Ground Effect

Ground effect occurs when the gliding height above the ground is lower than a wing span length. This effect is introduced in the drag coefficient, Eq.(7), by variation of an induced drag coefficient including a ground effect factor  $f(h)$ . The ground effect factor as a function of height, represented by Eq.(11), is plotted in Fig.2. From Fig.2, it is clear that the induced drag decreases when the height is lower than the wing span.

$$f(h) = \frac{33(h/b)^{3/2}}{1 + 33(h/b)^{3/2}} \quad (11)$$

## Wind Shear

Near the ground, wind speed varies due to the surface friction. This wind shear is defined by Eq.(12) where wind speed is assumed to be steady-state flow. Here,  $\kappa(\cong 0.4)$  is the Kalman constant,  $\delta(\cong 0.1)$  is the roughness coefficient, and  $U_w$  is the reference speed which relates to the speed  $u_{wr}$  at reference height  $H_r$ . Fig.3 shows a profile of wind shear where the reference height is  $H_r = 10[\text{m}]$ .

$$u_w = \frac{U_w}{\kappa} \ln \frac{h}{\delta} \quad (12)$$

$$U_w = \frac{u_{wr}\kappa}{\ln \frac{H_r}{\delta}} \quad (13)$$

## Optimal Control Problem

The optimal control problem for maximum range flight of the glider can be described as follows. State and Control :

$$\mathbf{X} = [u \ \gamma \ x \ h]^T \in \mathbb{X} \subseteq \mathbb{R}^4 \quad (14)$$

$$\mathbf{U} = [C_L] \in \mathbb{U} \subseteq \mathbb{R} \quad (15)$$

Minimize :

$$J = -x(t_f) \quad (16)$$

Subject to :

$$\text{Eq.(1) - (4)} \quad (17)$$

$$h \geq 0 \quad (18)$$

$$|C_L| \leq C_{Lmax} \quad (19)$$

here

$$\mathbf{X}(t_0) = [u_0 \ \gamma_0 \ x_0 \ h_0]^T \quad (20)$$

$$\mathbf{X}(t_f) = [free \ \gamma_f \ free \ h_f]^T \quad (21)$$

This optimal control problem has been solved by DIDO which is based on a Legendre pseudospectral collocation method.

According to the optimal control theory, the Hamiltonian value with respect to time and the final value of the co-states with respect to both inertial velocity and gliding range must be zero. These conditions are compared with the dual values composed by DIDO to check the optimality of numerical results.

## Numerical Results

Numerical simulation results are presented for four cases as shown in Table 1. The first three cases analyze maximum range flight for basic gliding (CASE A), ground effect (CASE B), and wind shear (CASE C), respectively, to obtain their individual characteristics. The final case analyzes a maximum range flight including the combination of both ground effect and wind shear (CASE D). Boundary conditions are  $u_0 = 22.5[\text{m/s}]$ ,  $\gamma_0 = 0[\text{deg}]$ ,  $h_0 = 30[\text{m}]$ ,  $\gamma_f = 0[\text{deg}]$  and  $h_f = 0[\text{m}]$ .

	Ground Effect	Wind Shear
CASE A	-	-
CASE B	○	-
CASE C	-	○
CASE D	○	○

Table 1 Cases of Numerical Simulations

The results are overlaid on a contour map of both energy height  $h_e$  and energy height consumption  $\dot{h}_e$  to analyze the individual characteristics. Here,  $h_e$  and  $\dot{h}_e$ , with respect to the ground-fixed coordinate system, are defined as Eq.(22)-(23).

$$h_e = \frac{1}{2g}u^2 + h \quad (22)$$

$$\dot{h}_e = \frac{1}{g}u\dot{u} + \dot{h} \quad (23)$$

Assuming  $\gamma$  is small, such as the case for a shallow glide, and  $C_L$  is the optimal lift coefficient obtained from Eq.(24),  $\dot{h}_e$  is reduced to Eq.(25).

$$C_{Lopt} = \sqrt{C_{D0}/k} \quad (24)$$

$$\dot{h}_e = -\frac{\rho S}{2mg}u u_a^2 (C_{D0} + kf(h)C_{Lopt}^2) \quad (25)$$

### CASE A: Basic Gliding Without Ground Effect and Wind Shear

The case for basic gliding does not include ground effect or wind shear and is simulated with  $u_w = 0$  and  $f(h) = 1.0$  in the equations of motion (Eq.(1)-(4)). Fig.4 shows basic gliding with and without a path constraint on height ( $h \geq 0$ ). Here, it is clear that most of the gliding is due to the optimal lift coefficient obtained from Eq.(24). In the case without a path constraint on height, as indicated by the dotted line, the optimal trajectory glides under the final height and performs a transient maneuver to satisfy the final condition. In the case with a path constraint, indicated by the solid line, the optimal trajectory switches to level flight until the gliding velocity reaches stall speed. Fig.5 shows a contour map of energy height  $h_e$  and energy height consumption  $\dot{h}_e$  with the overlay of optimal trajectories. In this case, the energy height consumption does not vary with height. As seen by the dotted line, without the path constraint imposed, the trajectory first tracks the constant energy height consumption curve then switches to tracking the constant energy height curve in order to satisfy the final condition.

### CASE B: Optimal Trajectory in Ground Effect

The case of gliding with ground effect is analyzed here. This case is simulated with  $u_w = 0$  in the equations of motion. Fig.6 shows the optimal trajectories with and without ground effect. The optimal trajectory with ground effect, indicated by the solid

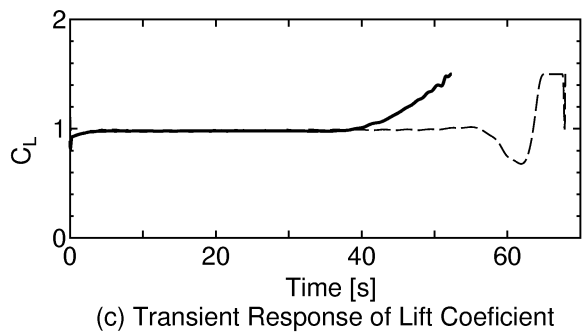
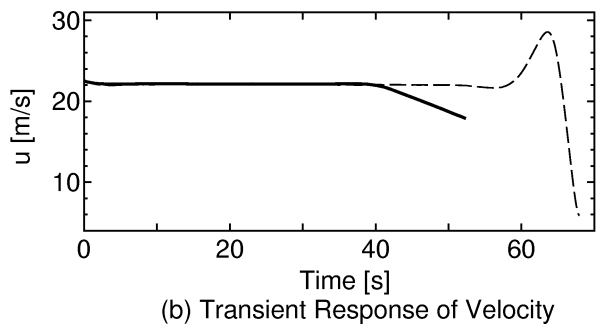
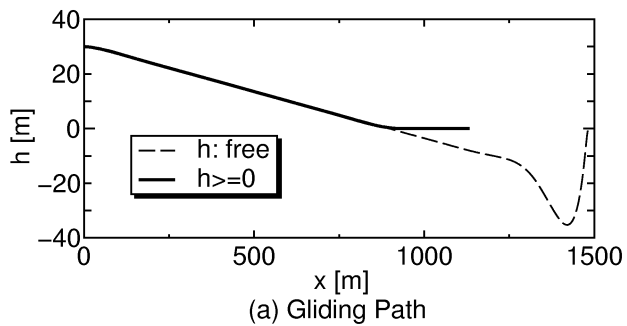


**Fig. 4 CASE A: Optimal Solutions for Basic Gliding**

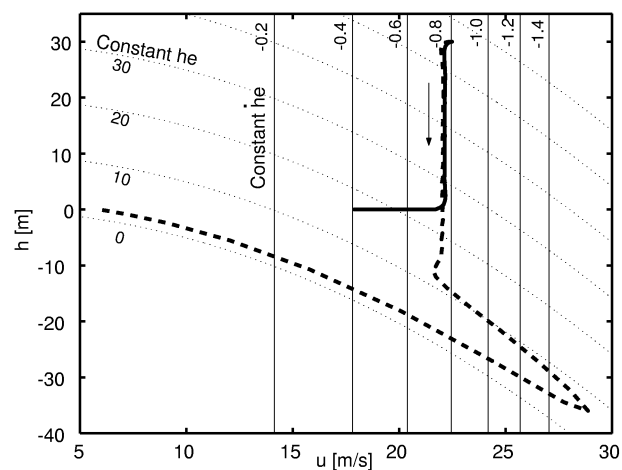


**Fig. 5 CASE A: Contour Map of Energy Height and Energy Height Consumption for Basic Gliding**

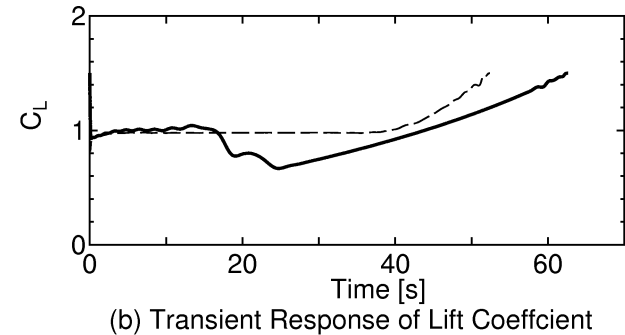
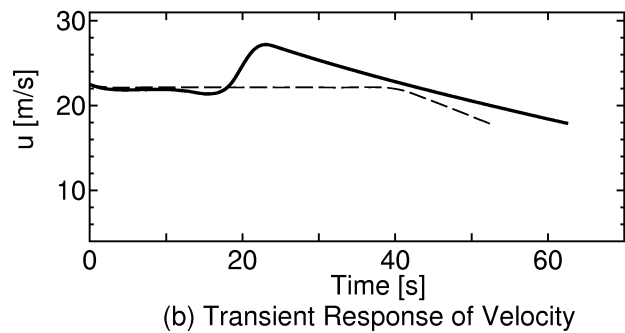
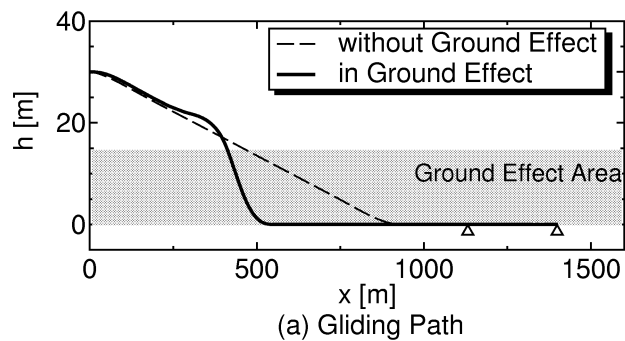


**Fig. 6 CASE B: Optimal Solution for Gliding with Ground Effect**

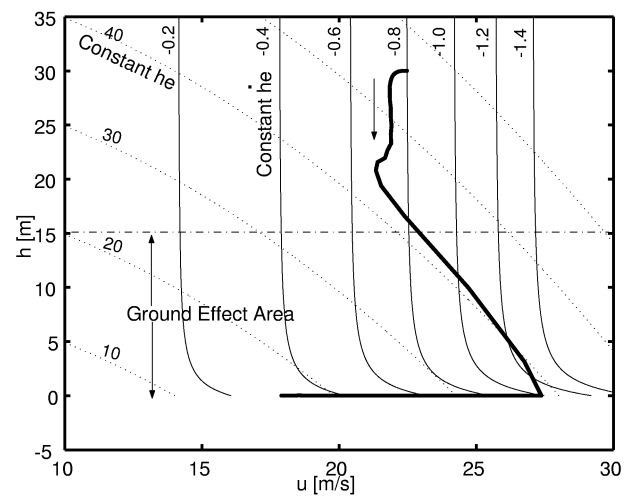


**Fig. 7 CASE B: Contour Map of Energy Height and Energy Height Consumption for Gliding with Ground Effect**

line, is using minimum altitude level flight rather than steady-state flight in the ground effect area. Fig.7 shows that the optimal trajectory is initially following the constant energy consumption height. In the ground effect area, the flight trajectory that diverges from the steady-state path results in improved energy consumption height compared to the same trajectory if allowed to proceed along the constant energy consumption contour.

### CASE C: Optimal Trajectory in Wind Shear

The case of gliding with wind shear is analyzed here. This case is simulated with  $f(h) = 1$  in the equations of motion. As seen in Fig.8, the optimal trajectories for variations in speed ( head wind / tail wind ) have a similar trend compared to the nominal no-wind trajectory ( $u_w = 0$ ). This contrasts the previous case ( Fig.6 ) where the trajectory without ground effect has a significantly different trend than the trajectory with ground effect. Fig.9 shows that the optimal trajectory in wind shear follows a constant energy consumption curve indicated by the  $\dot{h}_e$  contour.

### CASE D: Optimal Trajectory in Ground Effect and Wind Shear

This case combines both ground effect and tail-wind shear. Fig.10 shows the optimal trajectories for variations in wind speed. Fig.11 takes a closer look at the ground effect area. This figure shows that the optimal trajectory with wind tends to float more before reaching the minimum altitude ( $h = 0$ ). This phenomenon is caused by trade-off height between ground effect and tail wind shear. Fig.12 shows that the optimal trajectory is at first following a constant energy consumption curve as the case in Fig.9. When the glider comes down into the ground effect area, the trajectory resembles the ground effect case (Fig.7). However, Fig.12 shows that  $\dot{h}_e$  curves have a peak at low altitude, and that the optimal trajectory seems to follow the peak until the glider reaches the ground. Therefore, it is illustrated that the combination of ground effect and wind shear has an influence on the maximum range trajectory.

## Conclusions

The results of this paper demonstrate the importance of including ground effect and wind shear when analyzing maximum-range flight for a glider using optimal control theory. It was shown that the optimal trajectory depends on underlying energy management that is not obvious in the dynamical equations. Energy is not explicitly stated in any equations, yet the flight path demonstrates the vehicle will naturally try to conserve energy. The exclusion and inclusion of both wind shear and ground effect helps contrast the effects of this energy-dependent path.

These results can also be applied, but not limited to human-powered aircraft, reentry vehicle descent and landing, and any autonomous landing systems.

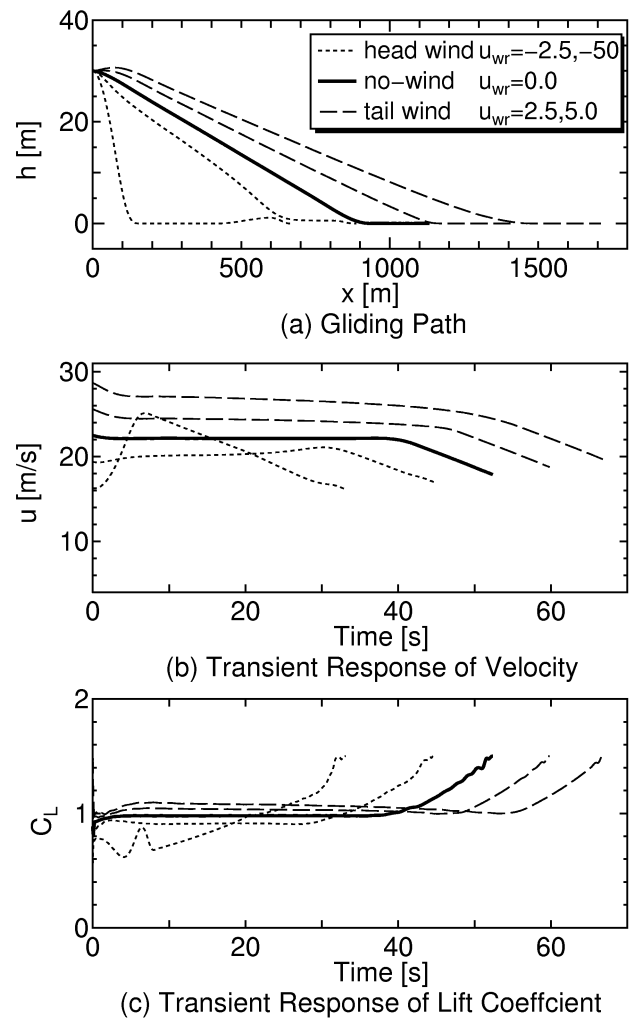


Fig. 8 CASE C: Optimal Solutions for Gliding with Wind Shear

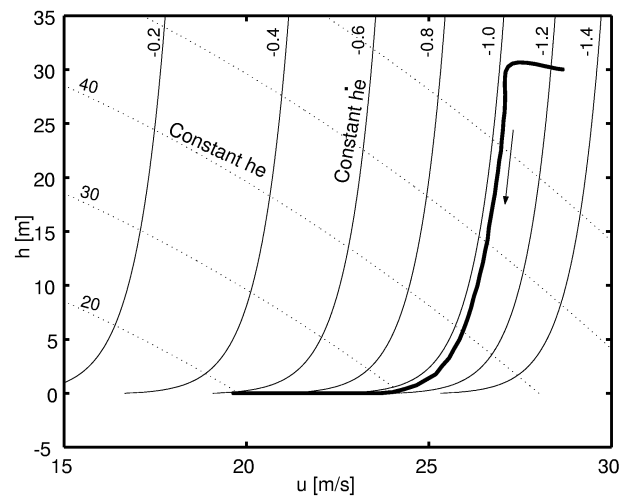


Fig. 9 CASE C: Contour Map of Energy Height and Energy Height Consumption for Gliding with Wind Shear

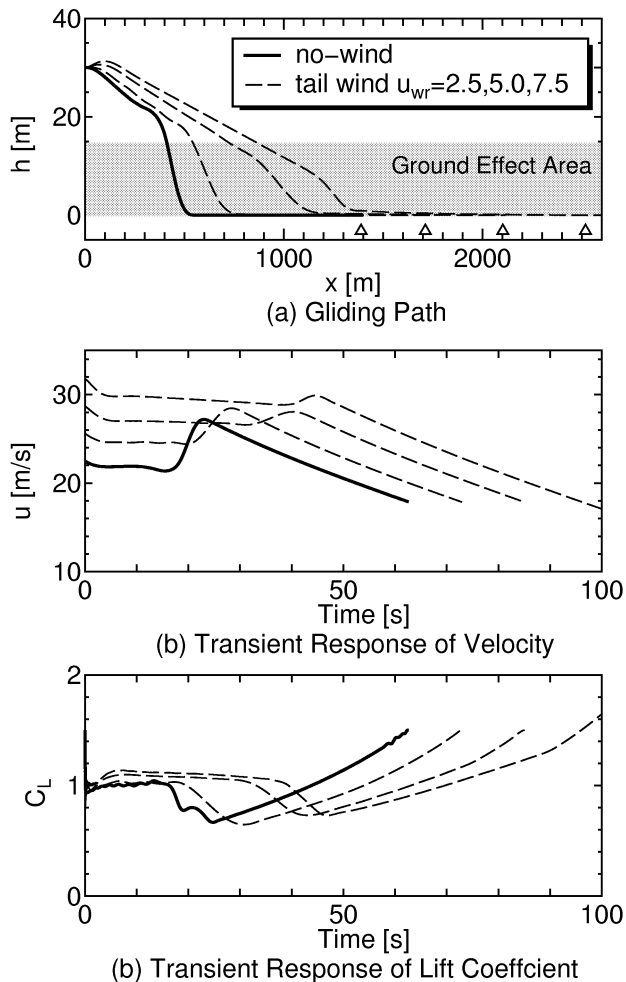


Fig. 10 CASE D: Optimal Solutions of Gliding with both Ground Effect and Wind Shear

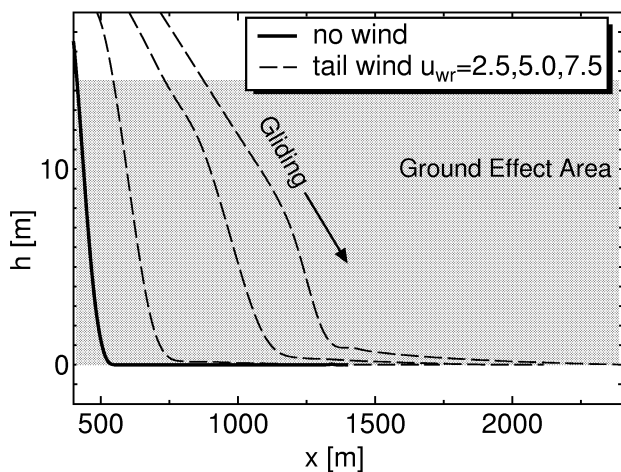


Fig. 11 CASE D: Optimal Trajectories in Ground Effect Area

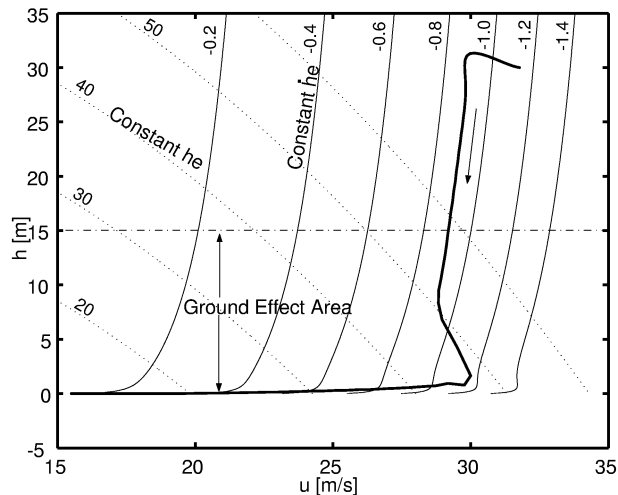


Fig. 12 CASE D: Contour Map of Energy Height and Energy Height Consumption for Gliding with both Ground Effect and Wind Shear ( $u_w = 7.5$  [m/s])

## References

- 1 Kluever, C.A., Unpowered Approach and Landing Guidance Using Trajectory Planning, *Journal of Guidance, Control and Dynamics*, Vol.27, No.6, 2004, pp.967-974.
- 2 Miyazawa, Y., Motoda, T. and Hata, T., Longitudinal Landing Control Law for an Autonomous Reentry Vehicle, *Journal of Guidance, Control and Dynamics*, Vol.22, No.6, 1999, pp.791-800.
- 3 Azuma A., The Biokinetics of Flying and Swimming, Springer-Verlag, Tokyo, 1992.
- 4 Langford J.S., The Daedalus Project, A Summary of Lessons Learned, *AIAA-8902048*, 1989, pp.1-10.
- 5 Heideman J.C. and Levy A., Sequential Conjugate-Gradient-Restoration Algorithm for Optimal Control Problems. Part1. Theory, *Journal of Optimization Theory and Applications*, Vol.15, No.2, 1975, pp.203-222.
- 6 Wu A.K. and Miele A., Sequential Conjugate Gradient-Restoration Algorithm for Optimal Control Problems with Non-Differential Constraints and General Boundary Conditions, Part1, *Optimal Control Applications & Methods*, Vol.1, 1980, pp.66-88.
- 7 Takano, H. A Study on Optimal Returns of an AOTV with the Limit of the Aerodynamic Heating, *Journal of Japan Society for Aeronautical and Space Sciences*, Vol.39, No.453, 1991, pp.522-530.
- 8 Takano, H. and Katoh, K., Maximum endurance flight of the Handlaunch, *Proceedings of the 20th Conference of JSASS*, 1989, pp.199-200.
- 9 Kawachi K., Inada Y. and Azuma A., An Optimal Flight Path of Flying Fish. *Journal of Theory and Biology*, Vol.163, 1993, pp.145-159.
- 10 Harada, M., Beppu, G. and Akira, A., A Study of Maximum Range Flight of Gliders, *Journal of Japan Society for Aeronautical and Space Sciences*, Vol.44, 1996, pp.582-587.
- 11 Ross, M., User's Manual For DIDO ( Ver. PR.1  $\beta$  ): A MATLAB Application Package for Solving Optimal Control Problems, *Technical Reports 04-01.0, Naval Postgraduate School*, 2004.